Supplementary information

Iron-based Electrocatalysts for Energy Conversion: Effect of Ball Milling on Oxygen Reduction Activity

Maida Aysla Costa de Oliveira [1], Pedro Pablo Machado Pico [1], Williane da Silva Freitas [1], Alessandra D'Epifanio [1], and Barbara Mecheri [1,*]

[1] Department of Chemical Science and Technologies, University of Rome Tor Vergata, Via della Ricerca Scientifica, 00133 Rome, Italy

* Correspondence: barbara.mecheri@uniroma2.it; Tel.: +39-06-7259-4488 (B.M.)

The FTIR spectrum of FePc (Figure S1a) shows a typical profile of metal phthalocyanines, with the strongest vibration bands in the range of 1800 and 600 cm^{-1}: $C_{arom.}$-H, C-N, and C=C stretching vibrations at 3058, 1467 and 1335 cm^{-1} respectively, C–H in-plane deformation (1158 cm^{-1}), symmetric vibrations of isoindole fragments (1120 cm^{-1}), C-H stretching (1083 cm^{-1}), in-plane deformation and Fe–N stretching (754 cm^{-1}) and $C_{arom.}$-H out-of-plane bending vibration at 727 cm^{-1} [1-3]. Table S1 reports the complete assignment of the vibrational bands in the FTIR spectrum of FePc. The FTIR spectrum of urea (Figure S1c) shows typical vibration bands due to N–H (3440 - 3350cm^{-1}) and C=O stretching (1677 cm^{-1}), N-H (1632 cm^{-1}) and C=O/NH_2 deformation (1603 cm^{-1}), C-N stretching (1478 cm^{-1}) and C=O wagging at 790 cm^{-1}, as previously reported [4-5]. Table S2 reports the complete assignment of the vibrational bands in the FTIR spectrum of urea. Figure S1b show FTIR spectrum of the FeNC_BM1 catalyst as comparison, showing all the vibration bands of urea, and three main contributions of FePc at 1334, 1119, 728 cm^{-1}.

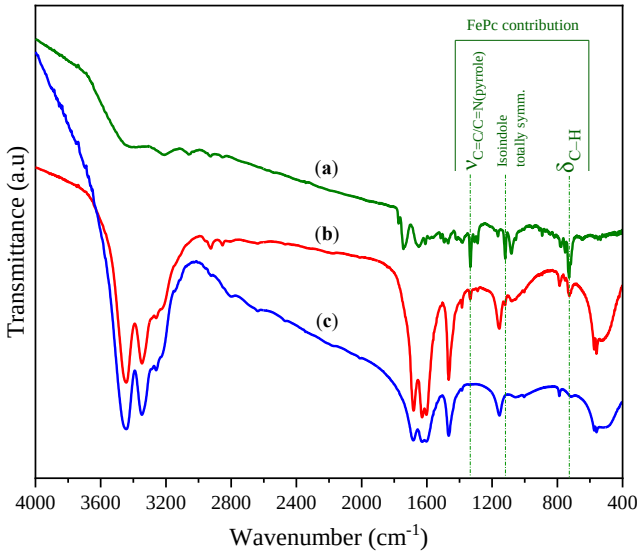

Figure S1. FTIR spectra of (**a**) FePc, (**b**) FeNC-BM1 catalyst, and (**c**) urea.

Table S1. Characteristic IR bands of iron (II) phthalocyanine.

Iron (II) phthalocyanine (FePc)	
Wavenumber (cm^{-1})	**Vibration**
3058	ν ($C_{arom.}$–H)
1467	ν (C=N) pyrrole
1335	ν (C=C) pyrrole
1158	δ (C–H) in-plane + isoindole
1120	Isoindole totally symm. vibration
1083	ν (C-H)
754	δ (C-H) in plane of isoindole / ν (Fe-N)
727	δ ($C_{arom.}$–H) out-of-plane

Table S2. Characteristic IR bands (cm^{-1}) of urea.

Wavenumber (cm^{-1})	**Vibration**
3443	ν (N-H)
3347	ν (N-H)
1687	ν (C=O)
1632	δ (N-H)
1603	δ(C=O)/(NH_2)
1478	ν (C-N)

Figure S2 shows the diffractograms of the organic precursors used as a source of Fe, N and C, which are in are in good agreement with the literature [6–8], while Figure S3 shows a direct comparison of intensity-normalized X-Ray diffractograms of FeNC_BM1 and FeNC_BM6.

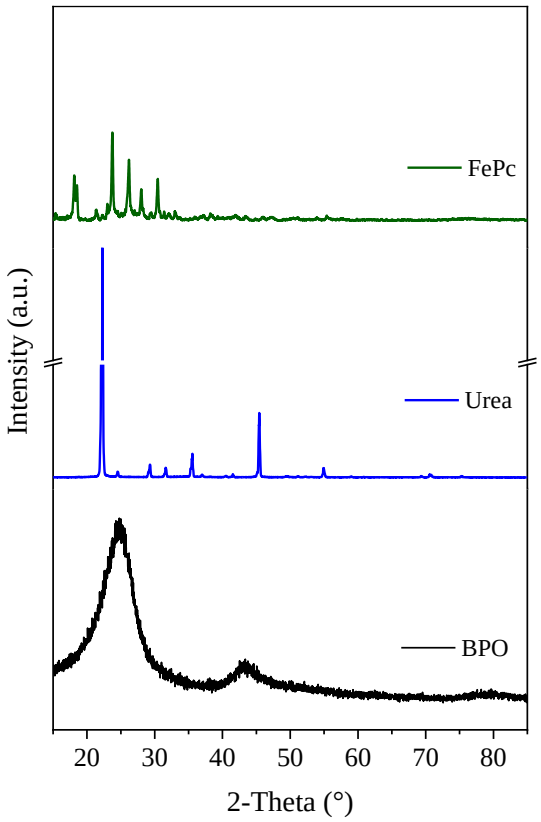

Figure S2. XRD patterns of BPO, urea and FePc.

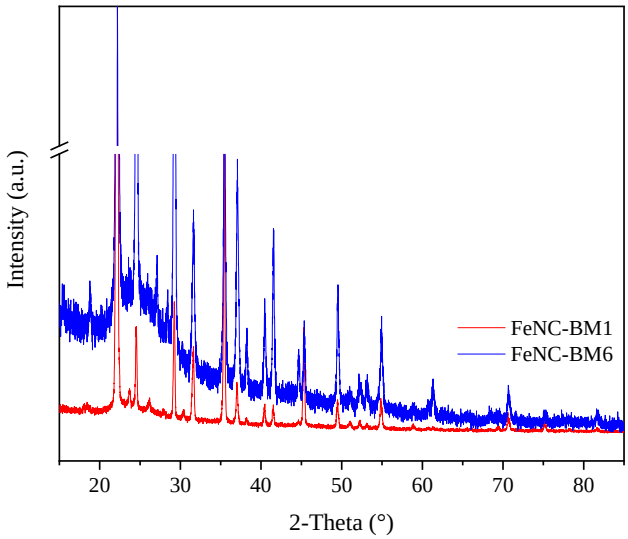

Figure S3. XRD patterns of FeNC_BM1 and FeNC_BM6 of FeNC_BM1 and FeNC_BM6.

References

1. Ziminov, A. V.; Ramsh, S.M.; Terukov, E.I.; Trapeznikova, I.N.; Shamanin, V. V.; Yurre, T.A. Correlation dependences in infrared spectra of metal phthalocyanines. *Semiconductors* **2006**, *40*, 1131–1136, doi:10.1134/S1063782606100022.

2. Zanguina, A.; Bayo-Bangoura, M.; Bayo, K.; Ouedraogo, G. V. IR and UV-visible spectra of iron(II) phthalocyanine complexes with phosphine or phosphite. *Bull. Chem. Soc. Ethiop.* **2002**, *16*, 73–79, doi:10.4314/bcse.v16i1.20950.

3. Monteverde Videla, A.H.A.; Osmieri, L.; Armandi, M.; Specchia, S. Varying the morphology of Fe-N-C electrocatalysts by templating Iron Phthalocyanine precursor with different porous SiO2 to promote the Oxygen Reduction Reaction. *Electrochim. Acta* **2015**, *177*, 43–50, doi:10.1016/j.electacta.2015.01.165.

4. Piasek, Z.; Urbanski, T. BULLETIN de L'ACADEMIE POLONAISE DES SCIENCES Serie des sciences chimlques Volume X The Infra-red Absorption Spectrum and Structure of Urea. *Bull. L'Academie Org. Chem.* **1962**, *X*, 113–120.

5. Manivannan, M.; Rajendran, S. Investigation of Inhibitive Action of Urea- Zn 2 + System in the Corrosion Control of. *Int. J. Eng. Sci. Technol.* **2011**, *3*, 8048–8060.

6. Zhu, H.J.; Lu, M.; Wang, Y.R.; Yao, S.J.; Zhang, M.; Kan, Y.H.; Liu, J.; Chen, Y.; Li, S.L.; Lan, Y.Q. Efficient electron transmission in covalent organic framework nanosheets for highly active electrocatalytic carbon dioxide reduction. *Nat. Commun.* **2020**, *11*, 1–10, doi:10.1038/s41467-019-14237-4.

7. Zhou, T.; Wang, Y.; Huang, S.; Zhao, Y. Synthesis composite hydrogels from inorganic-organic hybrids based on leftover rice for environment-friendly controlled-release urea fertilizers. *Sci. Total Environ.* **2018**, *615*, 422–430, doi:10.1016/j.scitotenv.2017.09.084.

8. Gambou-Bosca, A.; Bélanger, D. Chemical Mapping and Electrochemical Performance of Manganese Dioxide/Activated Carbon Based Composite Electrode for Asymmetric Electrochemical Capacitor. *J. Electrochem. Soc.* **2015**, *162*, A5115–A5123, doi:10.1149/2.0181505jes.

9. Valvo, M.; Liivat, A.; Eriksson, H.; Tai, C.W.; Edström, K. Iron-Based Electrodes Meet Water-Based Preparation, Fluorine-Free Electrolyte and Binder: A Chance for More Sustainable Lithium-Ion Batteries? *ChemSusChem* **2017**, *10*, 2431–2448, doi:10.1002/cssc.201700070.

10. Jaouen, F.; Marcotte, S.; Dodelet, J.P.; Lindbergh, G. Oxygen reduction catalysts for polymer electrolyte fuel cells from the pyrolysis of iron acetate adsorbed on various carbon supports. *J. Phys. Chem. B* **2003**, *107*, 1376–1386, doi:10.1021/jp021634q.